Original Article
A novel HDAC11 inhibitor potentiates the tumoricidal effects of cordycepin against malignant peripheral nerve sheath tumor through the Hippo signaling pathway

Po-Yuan Huang, I-An Shih, Ying-Chih Liao, Huey-Ling You, Ming-Jen Lee

Department of Neurology, National Taiwan University Hospital, National Taiwan University College of Medicine, Taipei, Taiwan

Abstract: Neurofibromatosis type 1 (NF1) is an autosomal dominant neurocutaneous disorder. Clinically, the hallmarks of NF1 include skin pigmentation and cutaneous neurofibroma. Some NF1 patients develop plexiform neurofibroma (PN) since early childhood. Pathologically, PN contains abundant Schwann cells, blood vessels and connective tissues, which may transform into a malignant peripheral nerve sheath tumor (MPNST). MPNST is a highly invasive sarcoma without any effective therapy. Recently, both *in vitro* and *in vivo* studies showed that cordycepin can inhibit the growth of MPNST cells. Cordycepin causes cell cycle arrest at G2/M phase and downregulates the protein levels of α-tubulin, p53 and Sp1. Herein, the present study revealed that the HDAC11 inhibitor, FT895, can synergistically enhance the tumoricidal effect of cordycepin against MPNST cells *in vitro*. Treatment with the combination of cordycepin and FT895 reduced the size of MPNST in the xenograft mouse model. The combined treatment decreased the protein levels of α-tubulin and KIF18A, which may disrupt the microtubule organization leading to the mis-segregation of chromosomes and aneuploidy. Moreover, the expression levels of TEAD1 and its co-activator TAZ, the candidate proteins in hippo signaling pathway, were suppressed after combined treatment. Sequence analysis found a few binding sites for the transcription factor, TEAD1 in the promoter regions of *TUBA1B*, *KIF18A*, *TEAD1*, *TAZ*, *YAP*, *TP53* and *SP1* genes. ChIP-qPCR assay showed that the combined treatment decreases the binding of TEAD1 to the promoters of *TUBA1B, KIF18A*, *TEAD1*, *TAZ* and *YAP* genes in STS26T cells. The reduced binding to *TP53* and *SP1* promoters was also found in S462TY cells, which was further confirmed by immunoblotting. The down-regulation of these important transcriptional factors may contribute to the vulnerability of MPNST. In summary, HDAC11 inhibitor, FT895 can potentiate the tumoricidal effect of cordycepin to suppress the MPNST cell growth, which was probably mediated by the dysfunction of hippo-signaling pathway.

Keywords: FT895, HDAC11 inhibitor, cordycepin, MPNST, ChIP-qPCR, Hippo pathway

Introduction

Neurofibromatosis type 1 (NF1) is an autosomal dominant neurocutaneous disorder with a prevalence of 1 in 3,500 individuals worldwide. The hallmarks of NF1 are the skin pigmentation and the cutaneous neurofibroma which grows along the peripheral nerves and mainly comprises of Schwann cells. Besides the cutaneous tumor, about one in four NF1 patients can develop one or more plexiform neurofibroma(s) (PN) [1, 2]. The PN typically appears at early childhood, containing abundant Schwann cells, collagen tissues, and blood vessels surround-ing the entire nerve [3]. Most of the neurofibroma is benign, however, it can be transformed into a malignant sarcoma celled malignant peripheral nerve sheath tumor (MPNST). Patients with NF1 have a 5-13% life-time risk to develop an MPNST; the risk is even more higher in patients with a large plexiform neurofibroma [4, 5]. For the treatment of MPNST, surgical excision is the only method to cure this intractable condition; however, the procedure is usually limited due to the large size, the encasement of large vessels or vital organs, or early metastasis. There is no effective chemo- or radio-therapy and the five-year survival rate is

low. Thus, it remains an unmet medical need for the treatment of MPNST.

Histone deacetylases (HDACs) play a key role in transcription regulation by removing acetyl group at the lysine residue of histone and non-histone proteins. HDACs can be classified into four classes (class I-IV) [6]. It has been reported that aberrant expression of HDACs was found in various cancers, e.g., HDAC1 in prostate, gastric and breast cancers [7-9], HDAC2 in colorectal cancer [10], HDAC6 in breast cancer [11], HDAC11 in lung, pancreatic cancers, and lymphoma [12-14]. The differential expression of HDAC in cancers makes it as a potential target for cancer therapy. HDAC11 is a newly discovered HDAC, which is the only member in HDAC class IV. HDAC11 has diverse substrates including histone and nonhistone proteins. For example, it can regulate the binding affinity of E2F1 and E2F4 to the adrenodoxin reductase tumor suppressor (*ARH1*) protein by deacetylation in breast cancer cells [15]. Inhibition of HDAC11 could increase the expression of OX-40 ligand in Hodgkin lymphoma. The induced OX40L further inhibited the generation of IL-10 producing Tr1 cells; subsequently, the host immunity was shifted toward the favorable anti-tumor immune response [13]. In neuroblastoma cells, depletion of HDAC11 leads to arrest of cell cycle, i.e., cancer cells accumulated in G2/M phase with aberrant formation of spindle assemblies; consequently, the cells underwent apoptosis [16]. FT895 is an analog of N-hydroxy-tetrahydroisoquinoline-7-carboxamide, a highly selective inhibitor to HDAC11, which shows more than 1000-fold selectivity against other HDACs [17]. FT895 can inhibit the proliferation of JAK2-driven myeloproliferative neoplasm by blocking the JAK/STAT signal pathway [18]. In lung cancer, FT895 reduced the self-renewal of cancer stem cells from non-small cell lung cancer and inhibited the growth of drug-resistant cancer cell stem cells by suppressing Sox2 expression [19]. These studies suggested that FT895 might be a potential therapeutic agent for cancers. Our previous study showed that cordycepin inhibits the growth of MPNST cells via the suppression of Sp1, p53 and tubulin expression [20]. However, the cytotoxic effect to MPNST cells required a relatively high concentration of cordycepin and the susceptibility in MPNST cell lines was variable. To avoid the adverse reaction from cordycepin and enhance the suppression of MPNST cell growth, the combined treatment with a HDAC inhibitor serves as an alternative treatment strategy. In this regard, we examined whether there is any synergistic effect after the low-dose cordycepin treatment combined with the specific HDAC11 inhibitor, FT895. The study demonstrated that the combined treatment synergistically inhibits the proliferation of MPNST cells *in vitro* and *in vivo*. The cell cycle of the treated MPNST cells arrested at G2/M and S phases with significantly reduced the expression of tubulin protein. We also found that protein level of the transcription factor, TEAD1 and its co-activators TAZ and YAP1, were significantly reduced post the combined treatment. The details of transcription control after treatment were evaluated by ChIP-quantitative PCR and poly(A) tail length assays. Our results indicated that after the combined treatment, Hippo signaling pathway may involve in the induction of MPNST cell death.

Materials and methods

Cell culture

The S462TY cell line was a kind gift from Dr. Timothy Cripe (Nationwide Children's Hospital Columbus, OH) [21]. The MPNST cell lines, STS26T, T265 and ST8814 have been reported before [22] and were gifted from Dr. Nancy Ratner (Cincinnati Children's Hospital, Cincinnati OH). The cells were grown as described elsewhere [23]. sNF96.2 and Hs53T were purchased from ATCC and cultured according to ATCC's instruction. LinNF neurofibroma cells was the primary culture collected from the benign neurofibroma of a NF1 patient who had signed the inform consent. The cells were kept in humid incubator at 37°C with 5% CO_2. The sample used in this study was approved by the Institutional Review Board of National Taiwan University Hospital, Taipei, Taiwan.

Cell proliferation assay

To evaluate the cytotoxicity of FT895 and cordycepin, the cells were seeded onto the 96-well plates at a density of 2×10^5 cells/mL, the day before treatment. The cells were treated with different concentrations of FT895, cordycepin or the combination of both drugs for 48 hours. At the end of the treatment, 7.5 μL of MTT (3-(4, 5-dimethylthiazol-a-yl)-2, 5-diphenyl tetrazolium bromide) at the concentration of 5 mg/mL was added to each well, and cells were incubated for 3.5 h at 37°C. After incubation, 75 μL of DMSO was added to each well for 20 min at

room temperature to dissolve the precipitates, and the absorbance was recorded by plate reader at the wavelength of 590 nm. The viability was analyzed by comparison of the absorbance between treatment- and control-groups.

Western blot

Cells were lysed using RIPA buffer for the extraction of proteins. The bicinchoninic acid (BCA) protein assay was employed to determine the protein concentration. Equal amounts of the lysate protein were separated by SDS-PAGE followed by transferring to a PVDF membrane. After blocking with 5% skim milk for one hour at room temperature, the membrane was probed with the specific primary antibody overnight at 4°C. The primary antibodies include anti-β-actin (1:4000, 4967S, Cell Signaling Inc.), anti-α-tubulin (1:5000, 11224-1-AP, Proteintech Group, Inc, Rosemont, IL), anti-acetyl-α-tubulin (1:3000, GeneTex), anti-GAPDH (1:10000, 10494-1-AP, Proteintech), anti-histone H3 (1:2000, abcam), anti-histone H3ac (1:2000, Merck Millipore), anti-histone H3K9ac (1:2000, Cell Signaling), anti-TAZ (1:2000, Cell Signaling), anti-YAP1 (1:2000, GeneTex), anti-TEAD (1:2000, GeneTex), anti-KIF18A (1:2000, GeneTex), anti-HDAC6 (1:2000, GeneTex), anti-HDAC11 (1:2000, Cell Signaling), anti-ERK (1:2000, Cell Signaling) and anti-phospho-ERK (1:2000, Cell Signaling) antibodies. Then, the membranes were washed with PBS containing 0.1% Tween 20 and incubated with horseradish peroxidase-conjugated secondary antibody, anti-rabbit IgG-HRP (#A120-101P, Bethyl, Montgomery, TX) for two hours. The protein signals were detected using the enhanced chemiluminescence method and the snapshot images were captured by UVP BioSpectrum 810 Imaging System (UVP, Cambridge, UK).

Cell cycle analysis

The treated cells were harvested and washed with ice-cold PBS. Then, the cells were fixed by 70% ethanol at -20°C for one hour. The cells were centrifuged at 300xg for 5 min and incubated in 0.1% Triton X-100, 2 µg/mL of RNase A and 20 µg/mL of propidium iodide at room temperature for 30 min in the dark. The cells were filtered by 35 µm nylon mesh to remove aggregates before subjected to fluorescence-activated cell sorting (FACS) analysis (FACSVerse, BD Bioscience, USA). Exclusion of aggregates was carried out to gate the single cell population on pulse-W versus pulse-A plot. The phase analysis of cell cycle was to fit a Gaussian curve. The plot was drew and analyzed by FloJo version 10.

Xenograft mouse

The male Balb/c nude mice at age 4 weeks were purchased from the BioLASCO Experimental Animal Center (BioLASCO, Taipei, Taiwan). All procedures in animals were approved by Institutional Animal Care and Use Committee of National Taiwan University Hospital (20190122). The STS26T and S462TY cells (5×10^6) were prepared in 0.1 mL DMEM medium and mixed with 0.1 mL of Corning® Matrigel (Coring, NY, USA). The mixture was injected subcutaneously into the flank of each nude mouse. The tumor sizes were measured using calipers, and the tumor volumes were estimated according to the following formula: Tumor volume (mm^3) = maximum length (mm) × (perpendicular width $(mm)^2$)/2. As soon as the tumor reached a mean size of 100-150 mm^3, the mice were subjected to injections with total volume of 100 µL of PEG, 10 mg/kg (full dose) or 5 mg/kg (half dose) of cordycepin, 1 mg/kg (full dose) or 0.5 mg/kg (half dose) of FT895, and the combination of cordycepin and FT895. The injections were carried out three times a week via the tail vein injection for at least 20 days. The body weight was recorded and the tumor volume was assessed using a Vernier caliper regularly.

Gene-specific measurement of poly(A) length

To assess the poly(A) tail length of the candidate genes, we used poly(A) tail length assay kit (Affymetrix, 76455, Thermo Fisher Scientific) to analyze the length. The method is based on high resolution poly(A) tail (Hire-PAT) assay. The procedure was described before [20]. In brief, the guanosine and inosine (G/I) residues were annealed onto the 3' end of the mRNA isolated from the samples. The tailed-RNAs are reverse-transcribed using the newly added G/I tails as the priming sites. PCR amplification was performed using two primer sets: (1) a gene-specific forward and reverse primer set designed upstream of the polyadenylation site as a control and (2) a gene-specific forward primer and the universal reverse primer which is provided by the kit to generate a product including the poly(A) tail and the control amplicon. The primer sets used to detected gene-specific poly(A) tail length are as follows: *TUBA1B* (forwa-

rd, 5'-GAAGAAGGAGAGGAATACTAA-3'; reverse, 5'-GATGTTAATGACTTTACTTTGAG-3'), *ACTB* (forward, 5'-TGCTTTCGTGTAAATTATGTAATGC-3'; reverse, 5'-CATTTTTAAGGTGTGCACTTTTATTC-3'), *YAP1* (forward, 5'-ATTGTGGGTGTGCCTATCATA-AC-3'; reverse, 5'-GAAGAGTTTAAGGAAAGAAT-ATATTTGAAC-3'), and *WWTR1* (forward, 5'-TTGACAGAGACCATTTTCCTAACA; reverse, 5'-TGGAAGTTCAATTGTCTTTATTTTTC-3'). The gen-escan method was employed to observe the changes in the poly(A) tail length after treatment. The fragment size was calculated by interpolation, using the Peak Scanner software 2.0. The actual poly(A) length can be determined by the subtraction between the fragment size obtained from forward primer site to the 5'-juxta-polyadenylation reverse primer site and the fragment size from the same forward primer to the universal reverse primer site.

Chromatin immunoprecipitation (ChIP) assay

The ChIP assay was carried out following the manufacturer's protocol of the Pierce Magnetic ChIP Kit (Thermo Fisher Scientific™). In brief, the chromatin from the cells was digested with MNase and sheared by sonication to fragment with the size less than 400 bp. The fragments were centrifuged (9000×g) at 4°C for 5 min. Ten percent of the diluted supernatant (input) was collected and served as the control template. The sheared chromatin was then, immunoprecipitated with 5 μg of anti-acetyl histone H3 and anti-TEAD1 antibodies (Merck Millipore) overnight. Magnetic beads and magnetic separation device (Merck, Darmstadt, Germany) were employed to isolate the protein/DNA complexes from the crude chromatin mixture. After elution, the DNA from immunoprecipitated samples and the inputs were recovered by phenol/chloroform. The input DNA and antibody-bound chromatin DNA were then subjected to the quantitative PCR to semi-quantifying the DNA copy number. The primers to amplify a fragment at the promoter region of the *TUBA1B*, *KIF18A*, *TAZ*, *YAP1*, *TEAD1*, *TP53* and *Sp1* genes were designed. The primer sequences are as follows: TUBA1B (forward, 5'-CATTTC-ACGGTGCTTCGTC-3'; reverse, 5'-AAAGACACC-GACCAGGGAAT-3'), KIF18A (forward, 5'-CAG-GTGAAGAGACCCCACAT-3'; reverse, 5'-AGAGGT-GGAGTTTGGGTGTG-3'), TAZ (forward, 5'-GGCT-GTCATCCCAACACTTT-3'; reverse, 5'-CCAGACT-CAAGCGATTCTCC-3'), YAP (forward, 5'-ACAGG-GATAGCAGGGGTAGG-3'; reverse, 5'-GTGCGTC-TTCAGGTACAAGC-3'), TEAD1 (forward, 5'-GTC-CCGGACTAGGGAAACTG-3'; reverse, 5'-TGGAA-

GCCTGGGTTTCTTC-3'), TP53 (forward, 5'-CAG-GCTTCAGACCTGTCTCC-3'; reverse, 5'-AGTGCC-TATATCAGTGCTGGG-3'), SP1 (forward, 5'-GTC-TTTTTAGGCGGACACCA-3'; reverse, 5'-GGAGG-GACTTGCAGAAGAAA-3').

Immunofluorescence and confocal microscopy

Cells grew on Ibid tissue culture dishes (IB-81156, Ibidi) overnight, and then were treated with cordycepin, FT895 or the combination for 24 hours. Treated cells were washed with PBS twice and fixed in 4% paraformaldehyde for 30 min at room temperature (RT). Permeation was applied with 0.1% Triton X-100 for 10 min at RT. The coverslips were blocked in PBS containing 5% fetal bovine serum for 1 h at RT. For immunostaining, the primary antibodies, anti-tubulin, anti-YAP1 and anti-TAZ antibodies were added onto the slide and incubated overnight at 4°C. The cell nuclei were stained by incubation with DAPI for 10 min at RT, and the cells were mounted using mounting medium for microscopy. The confocal images of tubulin assembly were acquired with a Zeiss LSM 880 (Zeiss, Germany). The images for nuclear translocation of YAP1 and TAZ were assessed using EVOS M7000 imaging system (ThermoFisher Scientific, MA USA).

Statistics and data analysis

All the experimental values were presented as mean ± SEM (standard error of mean). The analysis was performed by using Graphpad Prism version 9. For statistical comparison of values in xenograft mouse and ChIP assay, the Student *t* test was employed. For the comparison of values in those cells with nuclear translocation, Chi-square test was employed. A *P*-value of less than 0.05 was considered to be significant.

Results

The differential cytotoxicity effect of HDAC11 inhibitor FT895 on the neurofibroma and MPNST cell lines

In order to assess the inhibitory effect of cell growth in neurofibroma and MPNST, the specific HDAC11 inhibitor, FT895 was applied to the cultures. The MTT assay showed that the concentration of IC_{50} of FT895 on the neurofibroma primary culture LinNF is 121.9 μM, and 77.16 μM for NF1-related MPNST, sNF96.2, and 58.49 μM for the sporadic MPNST, STS26T. However, the extent of IC_{50} is much lower in
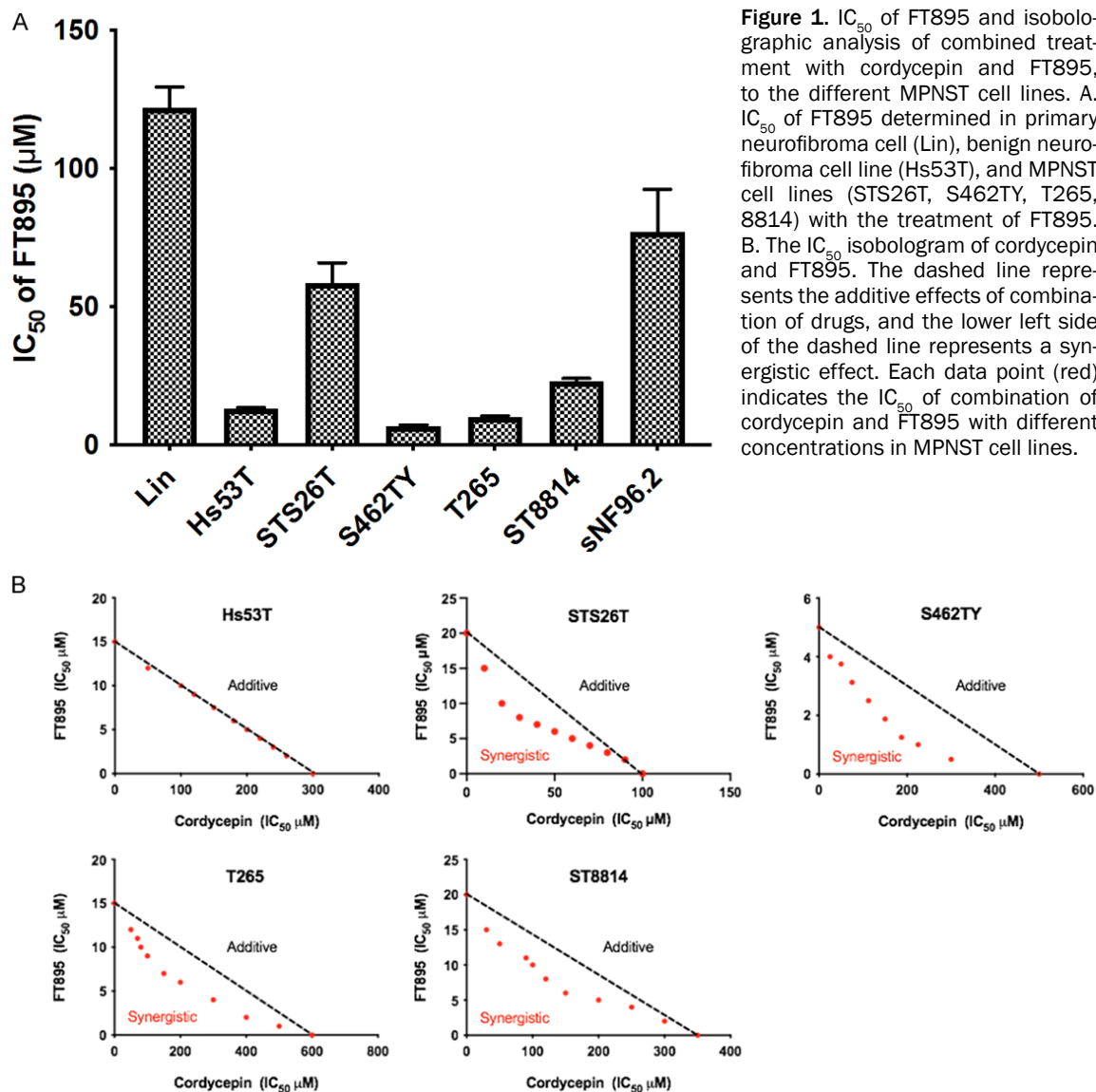
Figure 1. IC_{50} of FT895 and isobolographic analysis of combined treatment with cordycepin and FT895, to the different MPNST cell lines. A. IC_{50} of FT895 determined in primary neurofibroma cell (Lin), benign neurofibroma cell line (Hs53T), and MPNST cell lines (STS26T, S462TY, T265, 8814) with the treatment of FT895. B. The IC_{50} isobologram of cordycepin and FT895. The dashed line represents the additive effects of combination of drugs, and the lower left side of the dashed line represents a synergistic effect. Each data point (red) indicates the IC_{50} of combination of cordycepin and FT895 with different concentrations in MPNST cell lines.

neurofibroma cell line hs53T (13.12 µM) and MPNST cell lines, S462TY (6.76 µM), T265 (10.09 µM), ST8814 (22.88 µM) (**Figure 1A**). Among them, S462TY cells were most vulnerable to HDAC11 inhibition. These findings suggest that MPNST cell lines seem to be more sensitive to the administration of FT895.

Our previous work showed that cordycepin can inhibit the proliferation of MPNST cells, however, the dosage used to treat S462TY cells was relatively high, (IC_{50}, 768.6 µM) [20]. While considering enhancing the inhibition of cell proliferation with a lower concentration of cordycepin, the HDAC inhibitor, FT895 has been chosen as an add-on drug to evaluate whether there is any synergism on suppression of the cell growth of MPNST. The administration of FT895 re-

markably increased the sensitivity of S462TY and other MPNST cells to the treatment of cordycepin. The isobolograms showed a synergistic effect of the combination treatment to MPNST cells (**Figure 1B**). Nevertheless, there was only an additive effect in the benign neurofibroma cell line, Hs53T. These findings suggest that MPNST cells are sensitive to cordycepin treatment and FT895 can potentiate the inhibitory effect.

Cordycepin combined with FT895 induced aberrant chromosome positioning in the MPNST cells

Our previous study demonstrated that cordycepin can induce cell cycle arrest at the G2/M and S phases in the treated MPNST cells. The
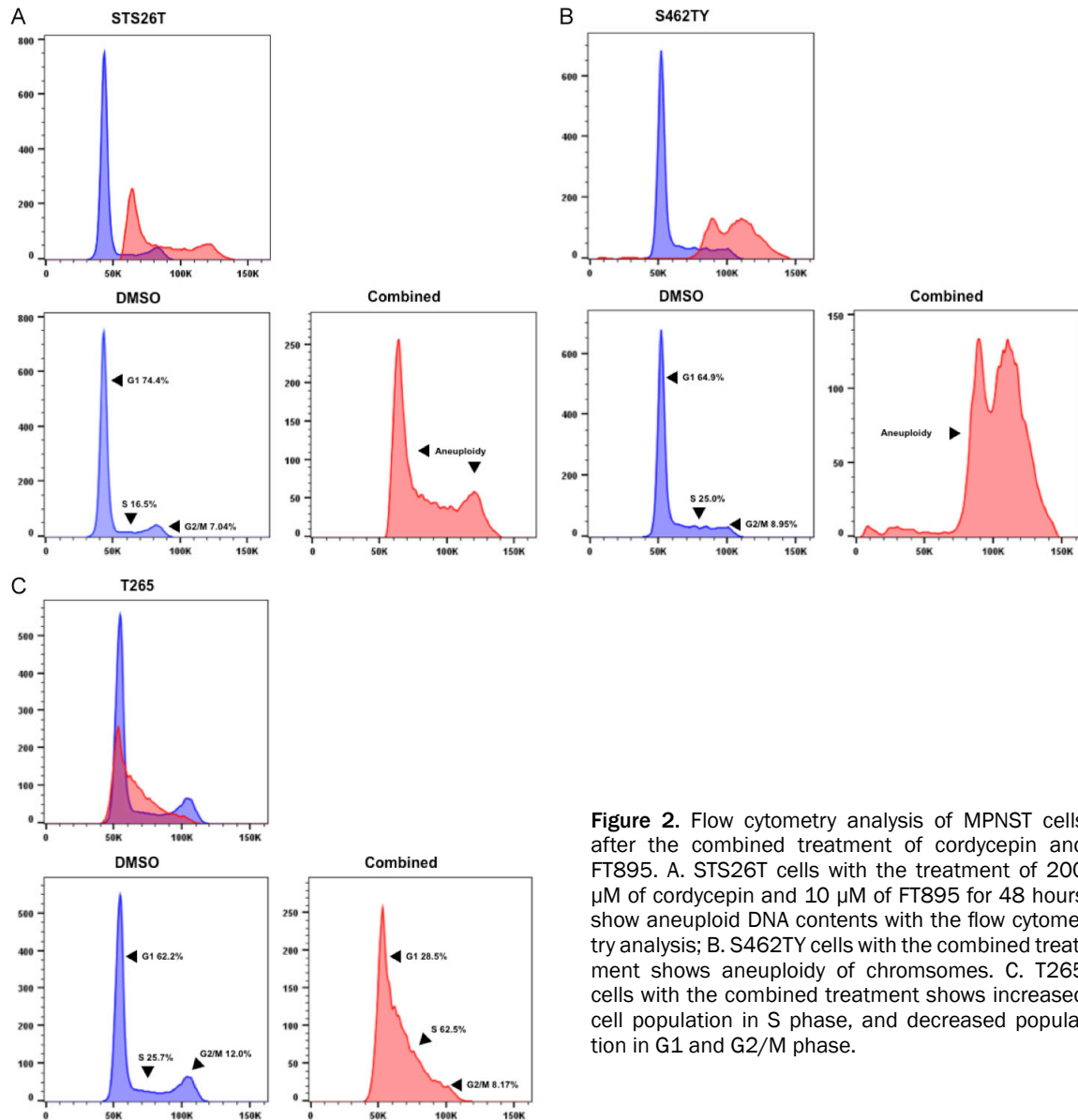
Figure 2. Flow cytometry analysis of MPNST cells after the combined treatment of cordycepin and FT895. A. STS26T cells with the treatment of 200 µM of cordycepin and 10 µM of FT895 for 48 hours show aneuploid DNA contents with the flow cytometry analysis; B. S462TY cells with the combined treatment shows aneuploidy of chromsomes. C. T265 cells with the combined treatment shows increased cell population in S phase, and decreased population in G1 and G2/M phase.

defects in tubulin and microtubule formation after treatment result in aberration of chromosome segregation during the process of replication [20]. Here, we found that the combined treatment of cordycepin (200 µM) and FT895 (10 µM) also induced the aberrant number of chromosomes in STS26T and S462TY, and cell cycle arrest in T265 MPNST cells. According to the flow cytometry analysis, the copy number of chromosomes was abnormal in STS26T and S462TY cells after treatment, more cells with aneuploid chromosomes at G1 phase in STS26T (**Figure 2A**) and with aneuploid at G2/M in S462TY cells (**Figure 2B**). While in T265 cells, the cell cycle was arrested at S phase after combined treatment (**Figure 2C**).

Albeit a less concentration of cordycepin (200 µM) used in the combination, the suppression of cell growth with abnormal cell cycle arrest and chromosome mis-segregation remains prominent in those treated MPNST cells. We previously reported that cordycepin can induce cell cycle arrest due to disruption of microtubule assembling. In order to investigate whether the combined treatment affect microtubule network as well, confocal microscopy was employed to detect its integrity. The crumple of tubulin leading to shrinkage of microtubules was observed (**Figure 3A**), and the network area was significantly dwindled in STS26T and S462TY cells after treatment (**Figure 3B**). These results suggested that the combination of
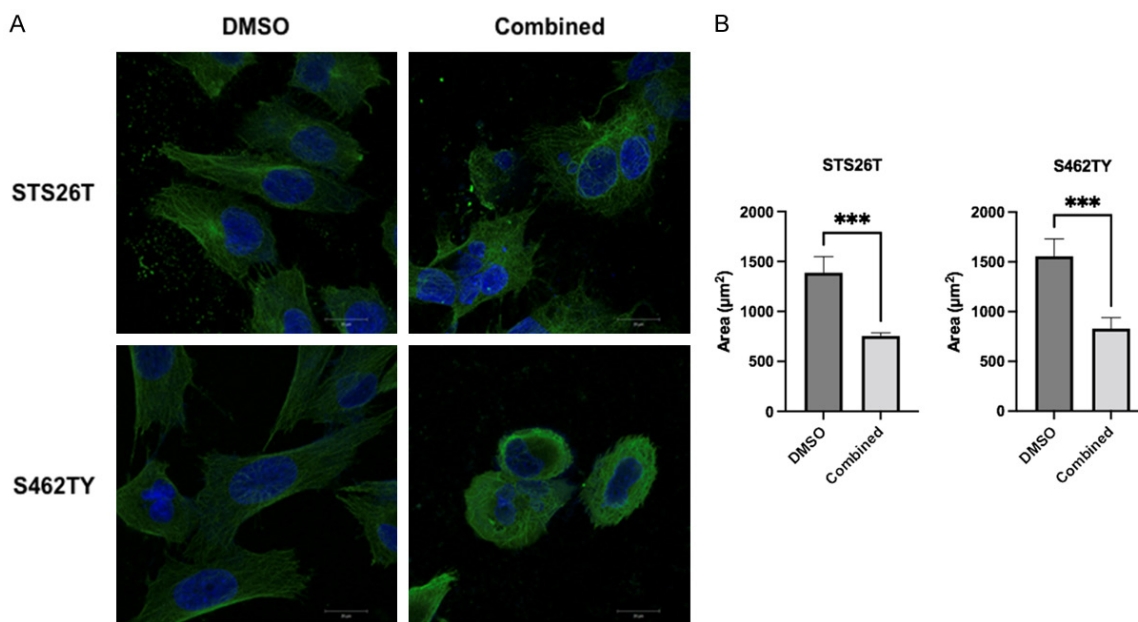
Figure 3. Impaired microtubule network in MPNST cells with the combined treatment of cordycepin and FT895. (A) Immunofluorescent image of α-tubulin (green) network in STS26T and S462TY cells after the treatment of DMSO (control group, left panel) or of the combination of 200 μM of cordycepin and 10 μM of FT895 (combined group, right panel). Blue color indicates DAPI staining. Scale bar, 20 μm. (B) The changes of microtubule area after the treatments were calculated from the green area of (A) by using image J. The student's *t*-test was employed to compare the microtubule network area between the DMSO and the combined group (***P<0.001).

cordycepin and FT895 spoils the integrity of microtubule network with the consequent impairment of mitosis. Mis-segregation of chromosomes with overloaded aneuploid MPNST cells after treatment results in further suppression of cell growth.

Combination of cordycepin and FT895 inhibited tumor growth in xenograft mouse model

While combined treatment of cordycepin and FT895 suppressed the MPNST cell proliferation *in vitro* in a synergistic manner, we further used xenograft mouse model to evaluate whether there is still an inhibitory effect of tumor growth *in vivo* post the combined treatment. The nude mice were subcutaneously inoculated with S462TY and STS26T cells. The 10 mg/kg of cordycepin (n=5), 1 mg/kg of FT895 (n=5) and the combination of cordycepin and FT895 (n=5) were intravenously (via tail vein) injected in every other day (**Figure 4A**). Compared to control group (n=4), all of the mice were tumor-free in the treatment groups after twenty-one days of treatment. However, there was no significant difference of tumor size among the treatment groups (**Figure 4B**). Given the synergistic effect of these two drugs and considering reducing the dose-related side effects, we fur-

ther employed cordycepin, FT895 and the combination with half the dose to treat the inoculated xenograft mice. The 5 mg/kg of cordycepin (n=5), 0.5 mg/kg of FT895 (n=5) and combined treatment (n=5) were given to the mice with inoculation of S462TY cells in every other day (**Figure 4C**). And to preclude the cell-line specific effect, some more mice were subjected to inoculate the STS26T cells and were only received the combination therapy. All of the mice with S462TY or STS26T inoculation were tumor-free at the end of treatment (**Figure 4D** and **4E**). However, the volume of S462TY tumor was reduced significantly quick in the combined treatment group than those with cordycepin or FT895 treatment alone at the treatment days (**Figure 4D**). The mice in the combined treatment group became tumor free in 24 days; however, it took 34 days in those mice treated with either cordycepin or FT895 alone. No tumor recurrence was observed after the treatment stopped (30 days of observation). These *in vivo* findings in the xenograft mouse model validate the synergistic effect observed in the *in vitro* study. Since cordycepin is a small molecule (M.W.=251.24 g/mol), the bioavailability of cordycepin given by intrperitoneal route would be close to that given by intravenous route [24]. In our previous study, a higher dose

A

S462TY with 10 mg/kg of cordycepin,
1 mg/kg of FT895 and combined treatment
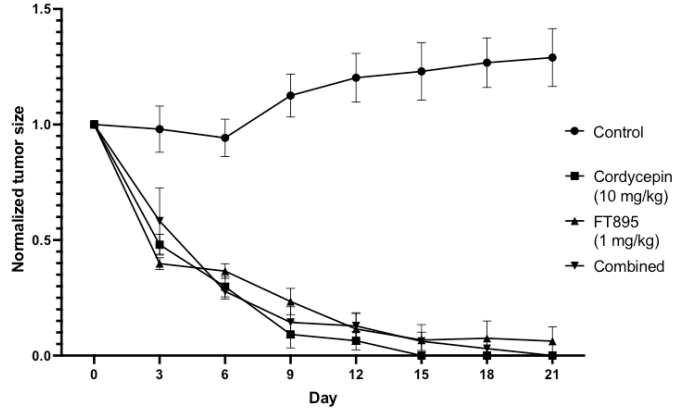
C

S462TY with 5 mg/kg of cordycepin,
0.5 mg/kg of FT895 and combined treatment
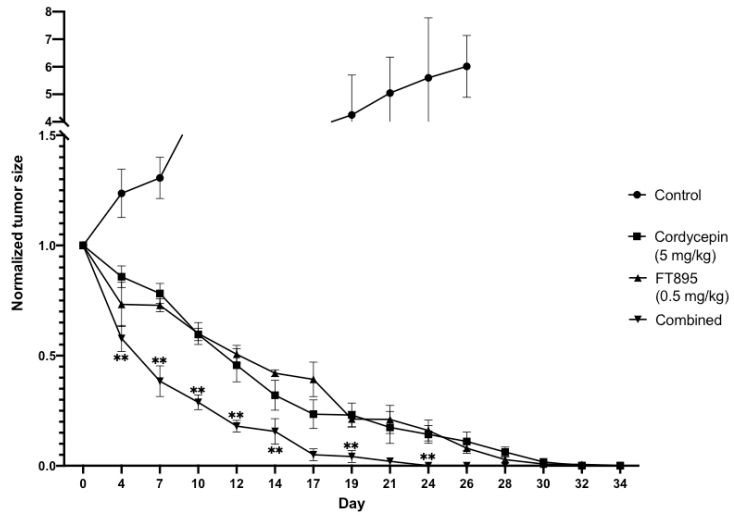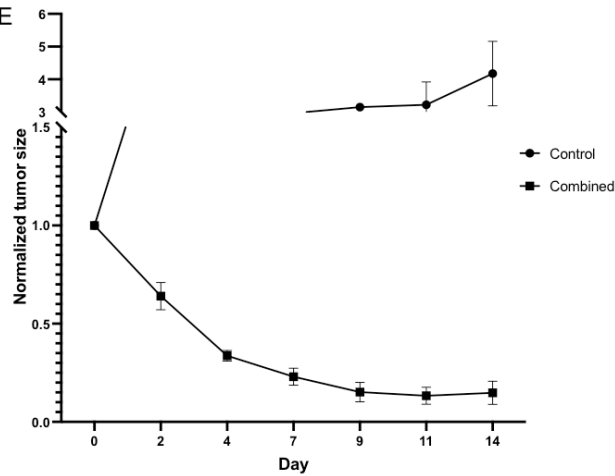
Figure 4. Tumor size of the xenograft mouse model after treatment of cordycepin, FT895 or the combination of both. A. The nude mice bearing S462TY cells were divided to four groups: control (N=4), 10 mg/kg of cordycepin (cordycepin group, N=5), 1 mg/kg of FT895 (FT895 group, N=5) and the combination of cordycepin and FT895 (combined group, N=5). The nude mice received medications three times a week via tail vein injection. B. The tumor size was plotted as fold change by normalization to the tumor size of day 0. C. The nude mice bearing S462TY cells receive half dose of cordycepin (5 mg/kg, N=5), FT895 (0.5 mg/kg, N=5), the combination of cordycepin and FT895 (N=5), and control group (N=3). D. The normalized tumor size with half-dose treatment. The reduction of tumor size in combined group was much more than the cordycepin group and FT895 group (**P<0.01, student's *t*-test). E. The nude mice bearing STS26T cells were divided to control group (N=3) and combined group (5 mg/kg of cordycepin and 0.5 mg/kg of FT895, N=6). The tumor size was represented by the normalized tumor volume.

of cordycepin (67 mg/kg) was used in xenograft mouse model through intraperitoneal injection and only mild adverse effect was reported. The dosage of cordycepin used in this study (5 mg/kg) is much less than that used in intraperitoneal injection. In this study, there was no decrease of body weight in most of the xenograft mice during the course of treatment. The complete blood cell counts and biochemistry profile were also unremarkable in the mice of each treatment group. These results indicated that the combined treatment of cordycepin and FT895 is less toxic to the mouse.

Cordycepin and FT895 suppressed α-tubulin and KIF18A expression in MPNST cells

Given the aneuploidy and cell cycle arrest in MPNST cells treated with cordycepin and FT-9895, we further evaluated the expression levels of microtubule-associated proteins which affects proper segregation of chromosomes. In previous study, we reported that cordycepin can reduce the expression level of α-tubulin in MPNST cells [20]. The combination treatment of cordycepin and FT895 led to a similar effect on MPNST cells in the present study. Expression of α-tubulin was significantly reduced after the combined treatment, but not treated with FT-895 alone (**Figure 5**). Moreover, the concentration of cordycepin applied to S462TY in combined treatment (200 μM) was less than the one which we previously reported (300 μM). Considering the defect of cell mitosis, we next assessed the level of kinesin-like protein 18A (KIF18A) which regulates the chromosome positioning during segregation process. FT895 did not inhibit the KIF18A protein expression, however, the combined treatment markedly reduced the level of KIF18A in S462TY and STS26T cells (**Figure 5**) which may confer to the aneuploidy found in those treated cells. These findings suggested that combination of cordycepin and FT895 suppresses the protein expression of α-tubulin and KIF18A, which may destabilize the microtubule network and hamper the chromosome segregation.

In our previous study, cordycepin shortened the poly(A) tail length of *TUBA1B* in S462TY and STS26T cells, which leads to the mRNA instability with subsequently decrease of protein expression of α-tubulin [20]. Combined treatment of cordycepin and FT895 also affected the poly(A) tail length in both STS26T and S462TY cells, with more emphasis on STS26T cells (**Figure 6**).

Hippo pathway was affected after combined treatment of cordycepin and FT895

Activation of Hippo-TAZ/YAP signaling has been reported to be crucial to the tumorigenesis of MPNST [25]. In order to evaluate whether the combined treatment affects the Hippo pathway, we examined the protein levels of transcription factor TEAD1 and its associated proteins, TAZ and YAP1. FT895 or cordycepin reduced the TEAD1 expression, and the combined treatment further suppressed the level of TEAD1 in S462TY, STS26T and T265 cells (**Figure 5**). The TAZ expression was significantly decreased after the combined treatment, which is similar to that found in TEAD1. However, neither the single nor the combined treatment can affect the protein expression of YAP1 (**Figure 5**). Besides the Hippo signaling pathway, we also evaluated other molecular mechanism involving in the suppression of MPNST cells after treatment. Phosphorylated p38 MAPK protein was decreased in S462TY, STS-26T and T265 cells. Furthermore, the total p38 MAPK protein was also reduced in S462TY and STS26T cells after combined treatment (**Figure 5**). The total and phosphorylated ERK proteins were not affected (**Figure 5**). These results suggested that the combined treatment of cordycepin and FT895 involves the Hippo pathway which supports the MPNST growth.

The epigenetic control of the candidate gene expression post combined treatment

Since FT895 is the specific inhibitor of HDAC11, we then investigated the epigenetic modifica-
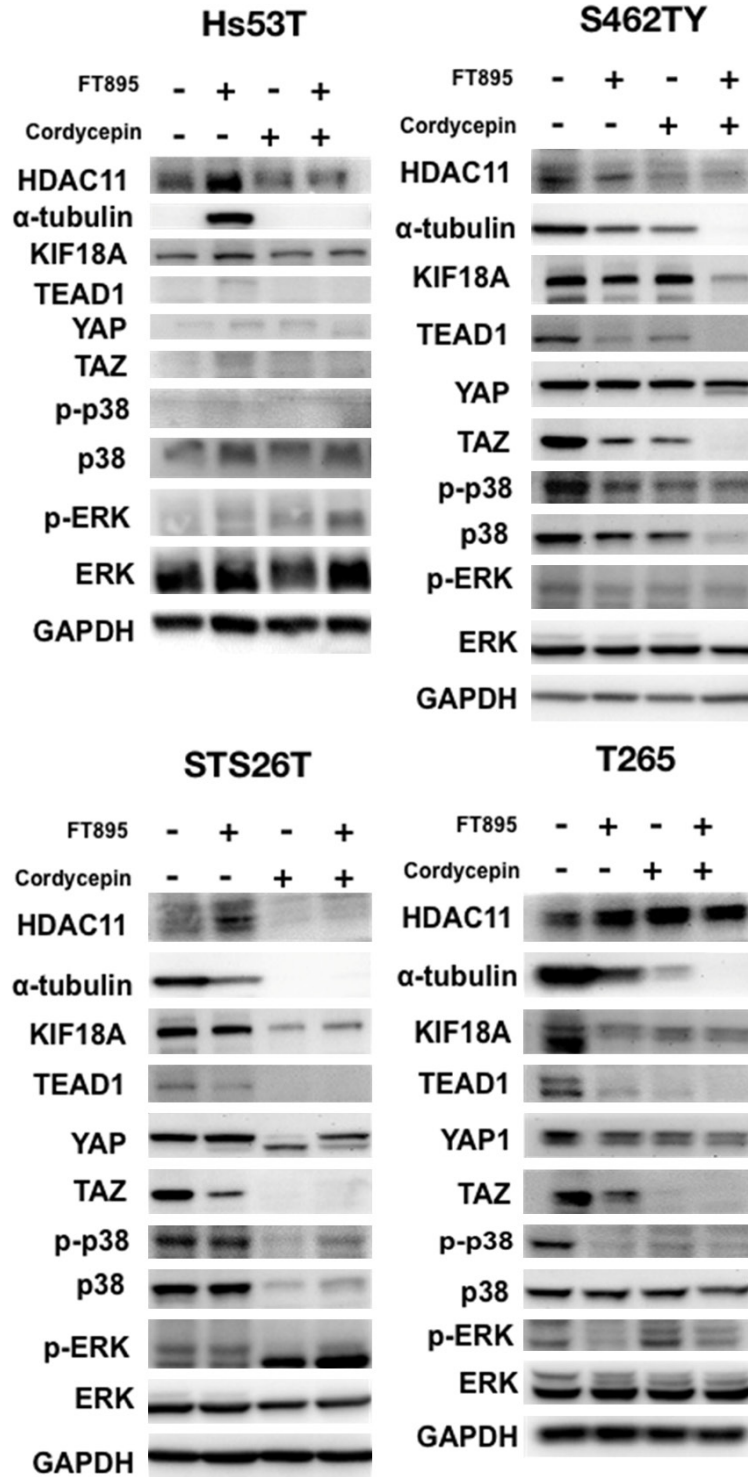
Figure 5. Western blotting for the specific protein levels in MPNST cells after treatment with 200 μM of cordycepin, 10 μM of FT895 and combination of cordycepin and FT895. Immunoblotting of HDAC11, α-tubulin, KIF18A, TEAD1, YAP, TAZ, total and phosphorylated p38, total and phosphorylated ERK, and GAPDH proteins in Hs53T, S462TY, STS26T and T265.

munoprecipitation (ChIP) with anti-acetyl histone H3 antibody was employed to pull down the transcriptionally active promoter region of the candidate genes. The copy number of promoter DNA has been semi-quantified using real-time PCR methodology. The evaluation of $\Delta\Delta C_T$ values showed that the level of active promoter region of *TUBA1B* and *KIF18A* gene was decreased in STS26T and S462TY cells, but remained unchanged in Hs53T cells after combined treatment (**Figure 7A**). The decrease of promoter DNA copy number which immunoprecipitated by anti-acetyl histone H3 suggest the inhibition of the transcription activity of *TUBA1B* and *KIF-18A* which was consistent to the decreased protein levels (**Figure 5**). Moreover, the levels of the active promoter regions of *TEAD1*, *YAP* and *TAZ* genes was also decreased in STS26T and S462TY cells, but not in Hs53T cells (**Figure 7B**). We also examined the copy numbers of active promoter DNA of *TP53* and *Sp1* genes binding to acetylated-histone 3. In our previous study, the protein levels of p53 and Sp1 were decreased after the cordycepin treatment. However, with the combined treatment of cordycepin and FT895, there is no significant difference between the control group and combined group (**Figure 7C**).

TEAD1 also known as transcriptional enhancer factor TEF-1, can bind to the M-CAT-like sequence motif (CATTCA/T) on the promoter region [26]. As shown in **Figure 8**, the M-CAT-like motif can be identified in *TUBA1B*, *KIF18A* and *TP53* promoter regions. Furthermore, the sequence motif can also be identified in the promoter region of *TEAD1* gene itself

tion on MPNST cells after the combined treatment of FT895 and cordycepin. Chromatin im-
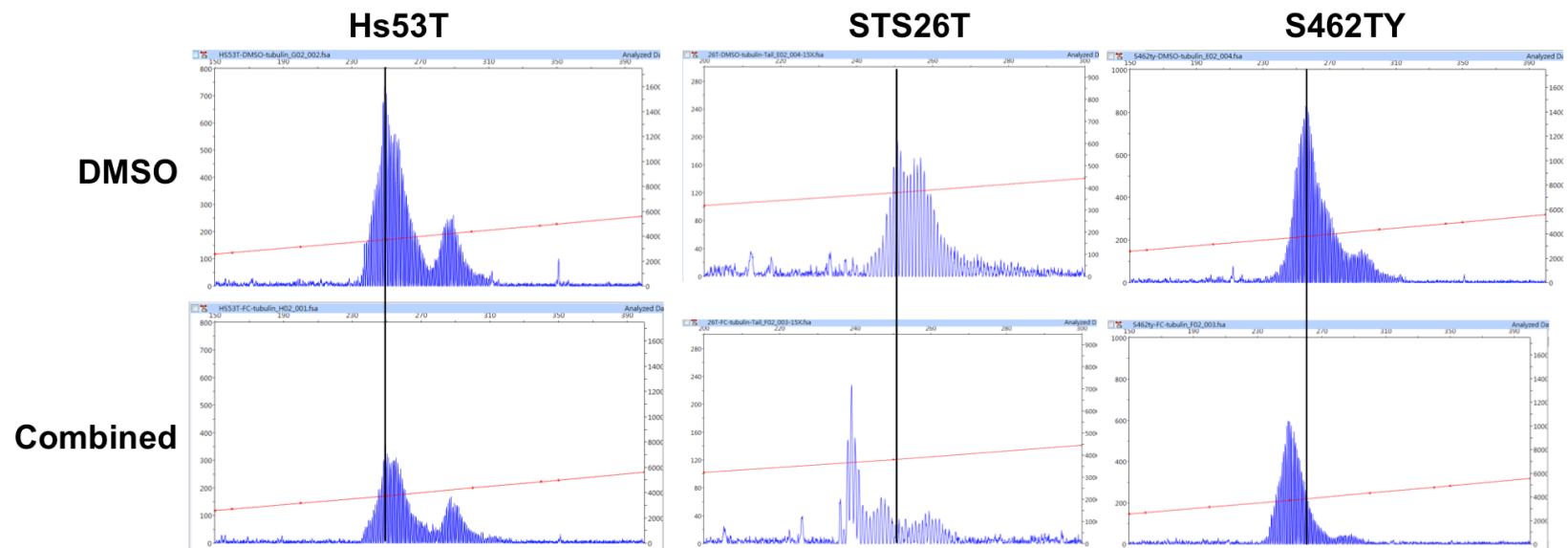
Figure 6. The poly(A) tail length of the mRNA of *TUBA1B* genes in Hs53T, STS26T and S462TY cells was measured and compared before and after combined treatment of 200 μM of cordycepin and 10 μM of FT895. The cluster of peaks, like shark teeth represents the poly(A) tails which were from the amplification of the 3'end and poly(A) of the candidate gene. The size of poly(A) tail length and the semi-quantitation of the PCR product were assessed using peak scanner software.
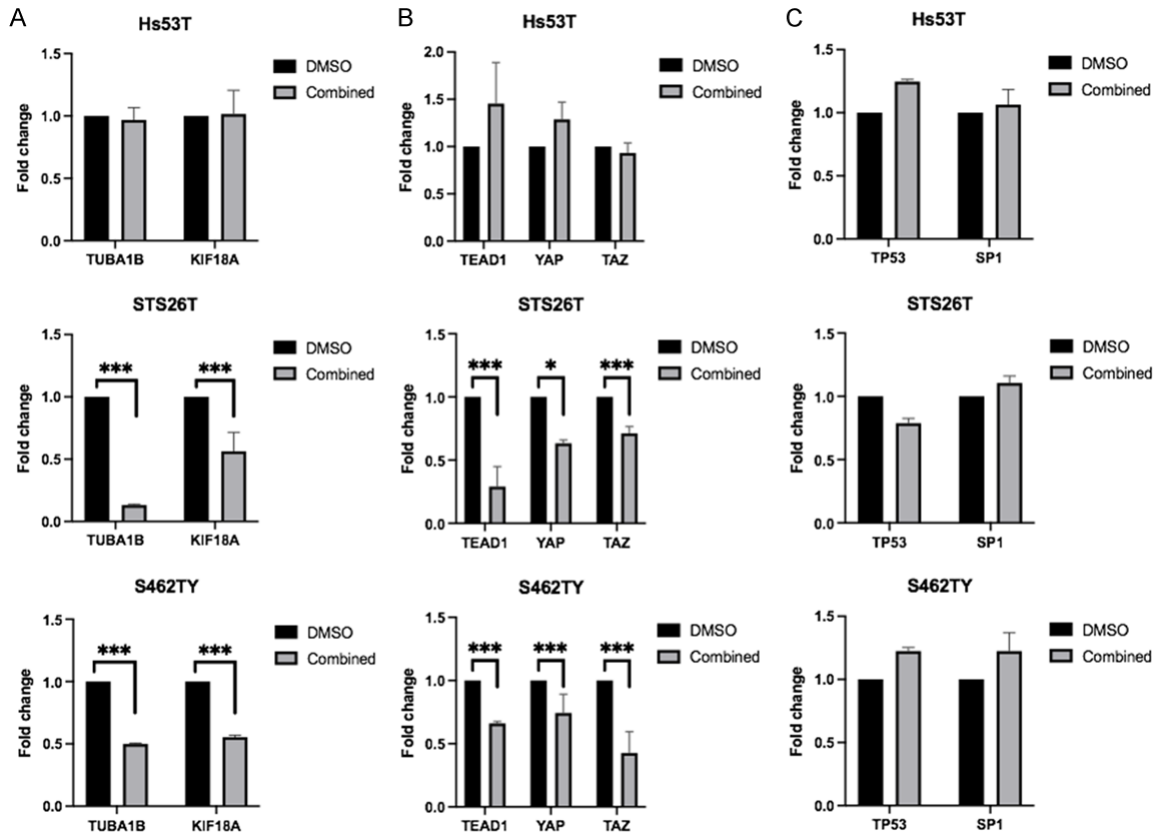
Figure 7. Transcription activity of microtubule associated proteins, hippo-signaling proteins and apoptosis-related protein in the MPNST cells after the combined treatment of cordycepin (200 µM) and FT895 (10 µM). Chromatin immunoprecipitation assay was employed using anti-acetyl histone H3 antibody to pull down the transcriptionally active promoter region. The copy number of promoter DNA was determined by using real-time PCR with specific primer pairs for *TUBA1B*, *KIF18A* (A, ***P<0.001), *TEAD1*, *YAP*, *TAZ* (B, *P<0.05, ***P<0.001), *TP53* and *SP1* (C). The fold change represents the copy number of combined group relative to the control (DMSO) group. The copy number of control group was considered as one hundred percent.

(**Figure 8**). Thus, the binding can facilitate its own transcription and there may be a self-regulated epigenetic control of expression in *TEAD1* gene. The M-CAT-like motif was also detected in the promoter regions in *YAP1* and *TAZ* genes which are the coactivator of TEAD1 in Hippo signaling pathway. These findings prompt us to envisage whether the transcription factor, TEAD1 can govern the transcription activity of the *TUBA1B*, *KIF18A*, *YAP1*, and *TAZ* genes. To evaluate the epigenetic control by the transcription factor TEAD1, chromosome-immuno-precipitation (ChIP) with anti-TEAD1 antibody followed by quantitative PCR (qPCR) to evaluate the copy number of promoter regions was carried out. ChIP-qPCR analysis showed that the DNA copy number of the promoter regions was decreased in *TUBA1B*, *KIF18A*, *YAP*, *TAZ*, and *TEAD1* genes in STS26T cells (F, but no chang-

es in S462TY cells after combined treatment (**Figure 9A** and **9B**).

Our previous study showed that cordycepin can inhibit MPNST cell growth through intervening the p53/Sp1 pathway. The promoter regions of *TP53* and *Sp1* genes also contain the M-CAT-like motif (**Figure 8**). To evaluate whether the combined treatment can epigenetically affected the expression of p53 and Sp1 through the Hippo signaling pathway, ChIP-qPCR analysis with anti-TEAD1 antibody has been performed. The copy numbers of *TP53* and *Sp1* promoter region binding to TEAD1, was reduced in S462TY cells, but not in Hs53T and STS26T cells after the combined treatment (**Figure 9C**). We further examined the protein levels of p53 and Sp1 in S462TY cells. By immunoblotting, combination treatment reduced the protein lev-
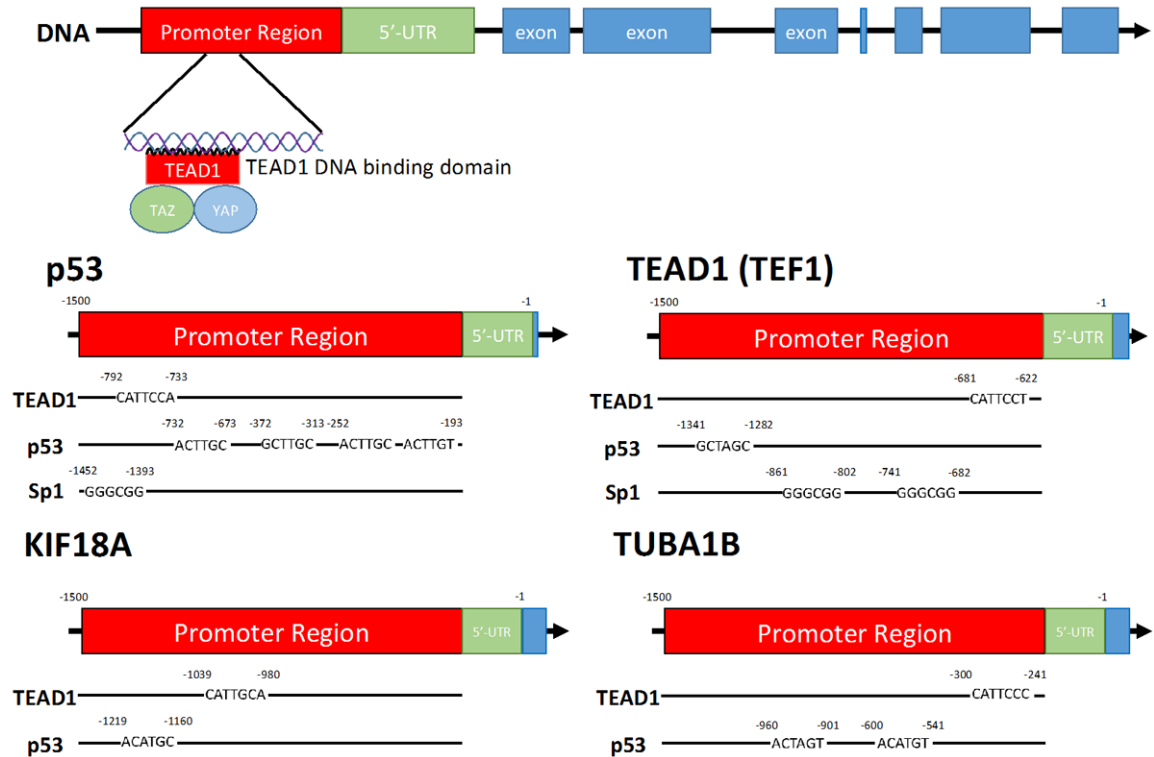
Figure 8. The binding motif of transcription factors, TEAD1, p53 and Sp1 found in the promoter regions of *TP53, TEAD1, KIF18A* and *TUBA1B* genes. The promoter region of p53 has three different binding motifs for TEAD1 (CATTCCA), p53 (ACTTGC) and Sp1 (GGGCGG). The binding motif sequences, TEAD1 (CATTCCT), p53 (GCTAGC) and Sp1 (GGGCGG) are found on the promoter region of TEAD1. The promoter region of KIF18A has two binding motifs, TEAD1 (CATGCA) and p53 (ACATGC). TUBA1B has TEAD1 (CATTCCC) and p53 (ACTAGT) binding motifs on its promoter region.

els of p53 and Sp1 in S462TY cells, but not in Hs53T cells (**Figure 10**). These findings are consistent to what we observed in the ChIP-qPCR results. These findings suggest that the combined treatment of cordycepin and FT895 can epigenetically suppress the expression of microtubule protein, KIF18A and Hippo signaling proteins. In addition, the expression level of p53 and Sp1 has also been reduced following the suppression of TEAD1 expression.

Treatment of cordycepin and FT895 increases the nuclear translocation of TAZ/YAP

Previous studies demonstrated that aberrant nuclear localization of TAZ/YAP correlates to tumorigenesis and drug resistance [27]. While considering the nuclear translocation may be a contributing factor for epigenetic control, we further evaluated whether the combined treatment can affect the nuclear translocation of TAZ/YAP protein in MPNST cells. As shown in **Figure 11**, the proteins, YAP and TAZ significantly translocated into nucleus in STS26T and S462TY cells (Chi-square test, P<0.0001), but not in Hs53T cells after the combined treatment. These findings suggested that the treatment can promote the nuclear translocation of TAZ/YAP; however, it seems that the translocation fails to bestow on its binding to the promoter regions of the candidate genes to enhance the transcription.

Discussion

Up to date, there remains no effective treatment for MPNST. In this study, we reported the synergistic effect of cordycepin and FT895 to inhibit the MPNST cell growth *in vitro* and *in vivo*. The addition of FT895, a specific HDAC11 inhibitor, remarkably increased the susceptibility of MPNST cells to cordycepin, especially in the S462TY cells. With combined treatment, the aneuploidy was observed in STS26T and S462TY cells, and the cell cycle was arrested at S phase in T265 cells. In our previous work,
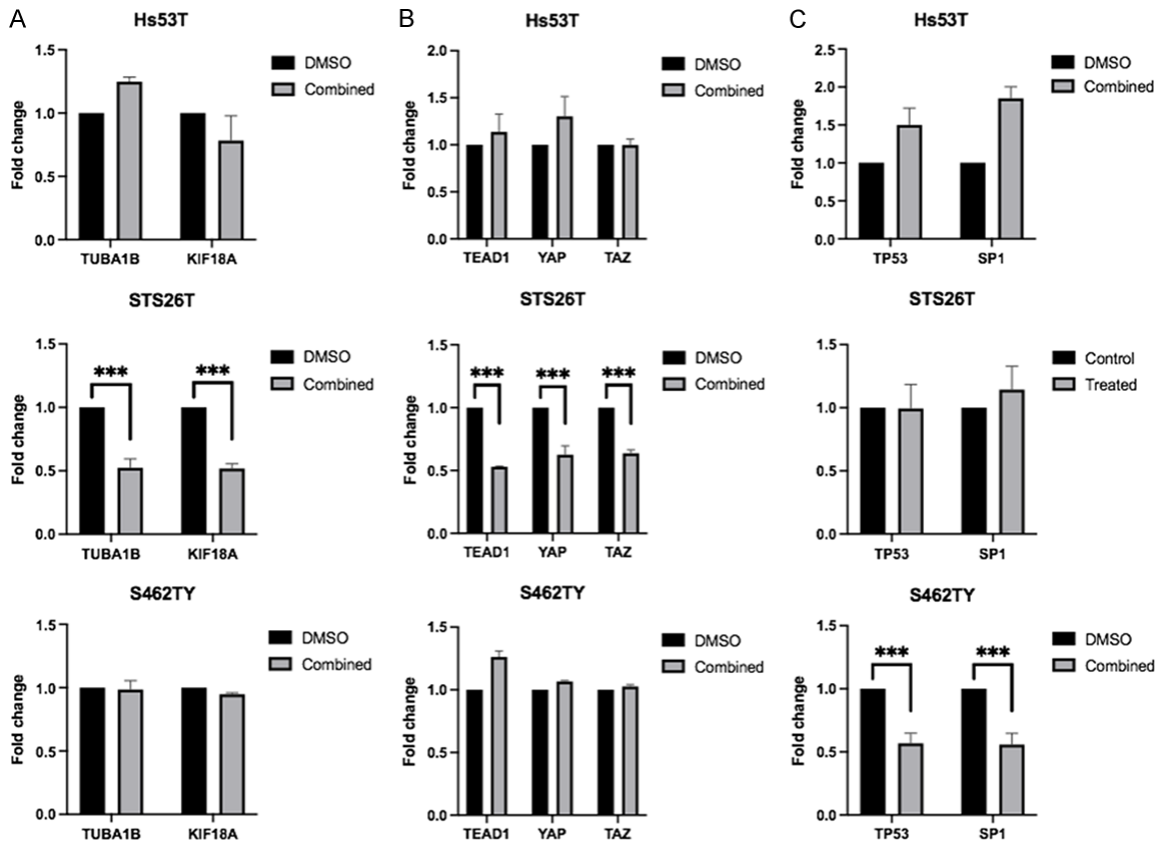
Figure 9. TEAD1 regulates the transcription of microtubule associated proteins, hippo-signaling proteins and apoptosis-related proteins in the MPNST cells after the combined treatment of cordycepin (200 µM) and FT895 (10 µM). Chromatin immunoprecipitation assay using anti-TEF1 (TEAD1) antibody to pull down the TEAD1 binding region on the promoter of candidate gene was employed. The copy number of promoter DNA was determined by real-time PCR methodology with specific primer pairs for *TUBA1B*, *KIF18A* (A, ***P<0.001), *TEAD1*, *YAP*, *TAZ* (B, ***P<0.001), *TP53* and *SP1* (C, ***P<0.001) genes. The fold change represents the copy number of combined group relative to that of control (DMSO) group, and the control group was considered as one hundred percent activity.
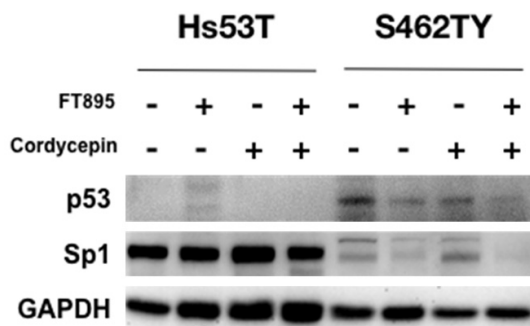
Figure 10. Protein levels of p53 and Sp1 after the treatment with 200 µM of cordycepin, 10 µM of FT895, and the combination of both drugs. The levels of p53 and Sp1 were decreased in S462TY cells after the combined treatment.

cordycepin compromised the microtubule network by reducing tubulin expression but not actin or GAPDH. The study demonstrated that the combined treatment of had a similar effect. Furthermore, the expression of KIF18A, a kinesin essential for chromosomal positioning during mitosis, was also suppressed in MPNST cells after combined treatment. The reduction of α-tubulin and KIF18A after treatment confers to the defective chromosomal segregation during mitosis which inevitably results in cell death. The *in vivo* study on xenograft mouse showed a significant inhibition of tumor growth with combined treatment (in half the dose) compared to the treatment of FT895 or cordycepin alone. Immunoblotting study demonstrated that the levels of TAZ and TEAD1 proteins reduced significantly after treatment. In addition, TEAD1 can bind to the promoter region of *TP53* and *SP1*. Reduction of TEAD1 led to less protein binding to the promoter of *TP53* and *SP1* in
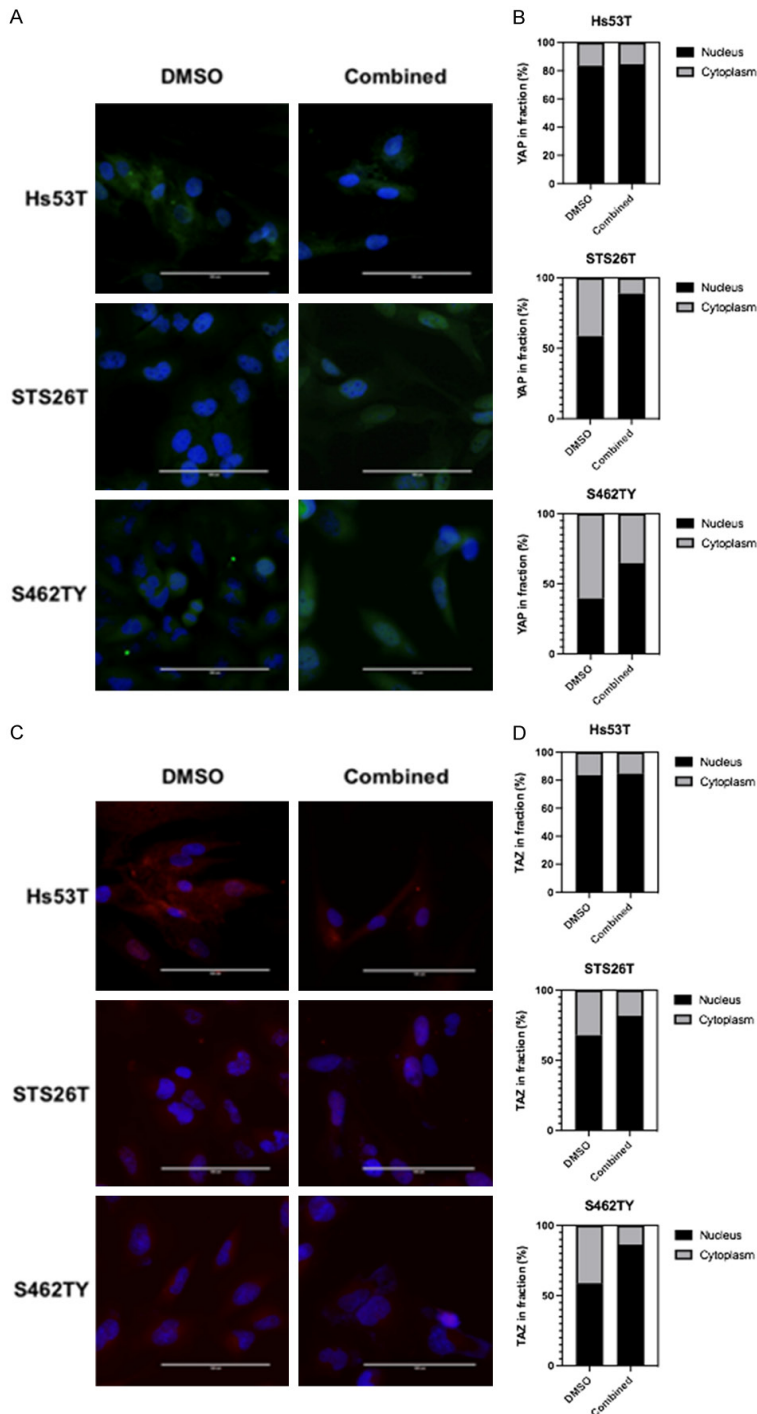
Figure 11. Nuclear translocation of YAP and TAZ after the combined treatment of cordycepin (200 µM) and FT895 (10 µM). A. Immunofluorescent image of YAP (green) and DAPI (blue) in Hs53T, STS26T and S462TY cells with treatment of DMSO and combination of cordycepin and FT895. B. Ratios of YAP expression in the nuclear and the cytosolic fraction in Hs53T, STS26T and S462TY cells. Combined treatment significantly induced nuclear translocation in STS26T and S4642TY, but not in Hs53T cells. C. Immunofluorescent image of TAZ (red) and DAPI (blue) in Hs53T, STS26T and S462TY cells with treatment of DMSO and combination of cordycepin and FT895. D. Ratio of TAZ expression in the nuclear and the cytosolic fraction in Hs53T, STS26T and S462TY cells. Combined treatment significantly trans-localizes the TAZ from cytoplasm to nucleus. Chi-square test was employed to compare between DMSO and combined groups.

S462TY cells. Consequently, the protein level of p53 and Sp1 was decreased in S462TY cells. **Figure 12** illustrates a possible molecular mechanism of growth inhibition in MPNST cells after the combined treatment.

HDAC11 is the newly discovered HDAC and the only member in HDAC class IV. Several reports have suggested that HDAC11 expression increases in many cancers [28, 29]. It has been reported that knockdown of HDAC11 leads to cell death as well as the inhibition of metabolic activity in colon, prostate, breast and ovarian cancer cell lines [30]. In addition, inhibition of HDAC11 activity suppressed the stemness of lung adenocarcinoma cells and reduced the viability of EGFR TKI resistance cells [19]. Therefore, specific HDAC11 inhibitor is a potential cancer therapy candidate. FT-895 is a highly selective inhibitor (IC_{50}=3 nM) for HDAC11 and is stable in serum ($t_{1/2}$=9.4 h in mouse) [17]. The application of FT895 to MPNST cells potentiates the inhibitory effect of cordycepin, and the significant synergistic effect was found in all MPNST cell lines *in vitro*. Similar effect was also observed on xenograft mouse model with full and half dose of cordycepin and FT895. In some pre-clinical studies, pan or selective HDAC inhibitor showed the enhancement of cancer therapy while combined with antitumor agents. For example, SAHA, a pan HDAC inhibitor approved by FDA, enhances the apoptosis and cell cycle arrest induced by cisplatin in lung cancer cell lines [31]. Selective class III HDAC inhibitor nicotinamide combined with doxorubixin increases the inhibition of cell proliferation
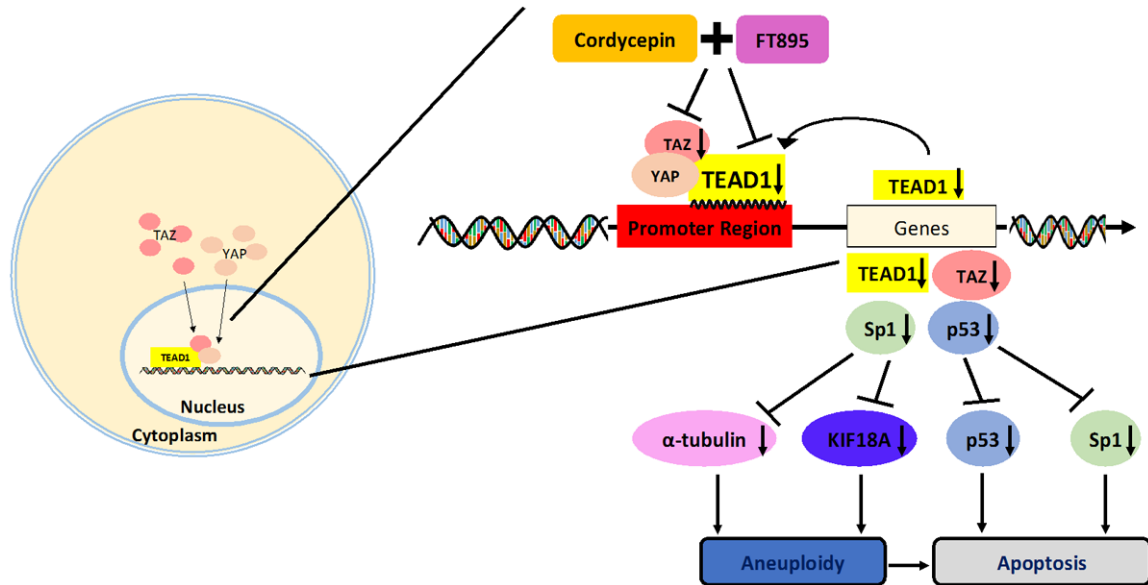
Figure 12. Molecular mechanism of combined treatment-induced growth inhibition in MPNST cells. Combination of cordycepin and FT895 reduces protein levels of TEAD1 and TAZ, which may further downregulate the transcription of α-tubulin, KIF18A, p53, Sp1 and even TEAD1 itself. Suppression of p53 and Sp1 causes apoptosis, and reduction of α-tubulin and KIF18A leads to abnormal number of chromosomes (aneuploidy). Self-regulation of TEAD1 can further reduce the expression of α-tubulin, KIF18A, p53 and Sp1.

and apoptosis in breast cancer cells [32]. These studies suggested that combination of HDAC inhibitor and chemotherapy not only enhances the tumoricidal effect but also reduces the dosage of anti-tumor agents, which can avoid the toxicity induced by chemotherapeutic agents.

Aneuploidy is toxic to cells by inducing proteotoxic and metabolic stress [33]. Aneuploidy arises from chromosome mis-segregation during cell division. Proper segregation of chromosome relies on the integrity of microtubule organization for fine-tuning of the process of chromosome segregation. Recent study suggested HDAC11 inhibition can interrupt the meiosis process in mouse oocyte and cause abnormal spindle microtubule organization by decreasing acetylated H4K16 and α-tubulin [34]. We previously reported cordycepin treatment can downregulate the expression of α-tubulin and perturb the progression of cell cycle in MPNST cells [20]. Our results indicated that FT895 alone or in combination with cordycepin can decrease the expression levels of α-tubulin and KIF18A proteins in MPNST cells. Loss of KIF18A results in aberrantly long mitotic spindle and loss of tension of kinetochores, which leads to the impaired chromosome alignment

[35]. Our study demonstrated that reducing the expression of α-tubulin and KIF18A might contribute to aneuploidy followed by apoptosis.

Aberrant activation of Hippo pathway has been considered as the hallmark of tumorigensis [36]. Wu *et al.* showed that human MPNST exhibits the upregulated TAZ and YAP proteins, and the activation of TAZ/YAP drives oncogenic transformation of Schwann cells. They used RNA interference targeting TAZ/YAP to inhibit the progression of MPNST [25]. These studies indicated that Hippo pathway may be a potential therapeutic target for the treatment of MPNST. In our study, combination of FT895 and cordycepin significantly suppressed TEAD1 and TAZ expression in MPNST cells. It has been reported that knockdown of TAZ can reduce the volume of tumor and inhibit metastasis in lung adenocarcinoma transplantation model [37]. Silencing the TAZ expression inhibits the proliferation of MCF10ACA1a TNBC breast cancer cell line [38]. These studies suggested that reduction of TAZ may contribute to inhibit the growth of cancer cells. The transcription factor TEAD1 involves in the downstream molecular mechanisms of Hippo, Wnt, TGF-β and EGFR pathways to induce EMT, metastasis and drug resistance in cancer cells [39]. TEAD1's coacti-

vators, TAZ and YAP are required for activation of Hippo signaling pathway. Since TAZ/YAP proteins do not bind DNA directly, we performed ChIP assay on the candidate genes which have the binding motif sequence of TEAD1 in their promoter regions. The copy number of promoter DNA binding to TEAD1 in *KIF18A*, *TUBA1B*, *TEAD1*, *TAZ* and *YAP* genes, indicate the efficiency of epigenetic control by the transcription factor, TEAD1. Among MPNST cells, STS26T were the only MPNST cells transcriptionally affected by the reducing level of TEAD1 after treatment. TEAD1 can bind its own promoter, which makes TEAD1 as a self-regulating transcription factor to control its own expression. Less expression of TEAD1 protein might decrease the available TEAD1 binding to its own promoter, with further decelerating or downregulating of the transcription. This self-regulating process may explain the vulnerability of MPNST cells to combined treatment. YAP protein was reported to be able to upregulate p53 protein by directly binding to the promoter of *TP53* [40]. Sequence analysis showed that *TP53* and *SP1* contain TEAD1 binding motifs on their promoter region (**Figure 8**). ChIP assay indicated that less DNA copy number of *TP53* and *SP1* promoter binds to TEAD1 protein in S462TY cells after treatment. Immunoblotting confirmed the decreased level of p53 and Sp1 proteins in S462TY which validates the downregulation of the transcription after treatment.

In our previous study, cordycepin exhibited the inhibition of MPNST cell growth via reducing expression of the transcription factors, p53 and Sp1 [20]. Cordycepin treatment decreased the levels of p53 and Sp1 proteins resulting in reduction of binding to the *TUBA1B* promoter. KIF18A has been reported to be a target of p53 signaling pathway by bioinformatics screen [41]. Sequence analysis reveals that the promoter region of *KIF18A* gene contains p53 binding motif. Loss of p53 protein expression was found in STS26T and T265 MPNST cells [20], which causes a much less binding to *KIF18A* promoter, and subsequently, reduces the expression of KIF18A protein. However, p53 protein level and the cell growth were not affected after cordycepin treatment in S462TY cells [20]. Hence, we hypothesized the less sensitivity to cordycepin in S462TY was possibly due to the unaffected p53 level. The results showed that the combined treatment reduces

the level of p53 in S462TY cells which may enhance the susceptibility of S462TY cells to cordycepin. S462TY carries a *TP53* mutation (c.329G>C), and shows abnormal nuclear accumulation [42]. The modulating effect of p53 might account for the differential sensitivity to the drugs. S462 cells (The parental cells of cell line S462TY) treated with combination of imatinib and erlotinib responded less to the therapy than the MPNST cells carrying wild-type p53 [43]. Although our results is disparate to the recent study which suggests that HDAC11 inhibition can enhance the p53 expression in pituitary tumor cells [44], there are several studies demonstrated that cancer cells may be differentially responded to HDAC11 inhibition [13, 16]. Translocation of TAZ and YAP is regulated by stress signal, including ER, oxidative ROS and osmotic stresses [45]. Here, we showed that translocation of TAZ and YAP from cytoplasm to nucleus is increased after combined treatment. The increased translocation could be a stress-induced reaction to the treatment for compensating the loss of TEAD and TAZ.

In summary, our results identify the potential of HDAC11 inhibitor FT895 to enhance the tumoricidal effect of cordycepin in MPNST cells and also provide a molecular mechanism for such an effect. Combination of cordycepin and FT-895 synergistically inhibits MPNST cell growth. The reduced α-tubulin and KIF18A protein expression, causes mis-segregation of chromosomes leading to cell apoptosis. Combination of cordycepin and FT895 also suppresses the expression of transcription factor TEAD1 and TAZ in Hippo signaling pathway which is essential for the growth of MPNST. Loss of TEAD1 transcriptionally downregulates the expression of *KIF18A*, *TUBA1B*, *TEAD1*, *TAZ* and *YAP* in STS26T cells, and *TP53* and *SP1* in S462TY cells. Our study highlights that FT895 can potentiate the inhibition of cordycepin which provide an alternative treatment strategy against MPNST.

Acknowledgements

Disclosure of conflict of interest

None.

Address correspondence to: Dr. Ming-Jen Lee, Department of Neurology, National Taiwan University Hospital, National Taiwan University College of Medicine, Taipei, Taiwan. Tel: +886-2-23123456 Ext. 65336; Fax: +886-2-23418395; E-mail: mjlee@ntu.edu.tw

References

[1] Friedman JM. Epidemiology of neurofibromatosis type 1. Am J Med Genet 1999; 89: 1-6.

[2] Lee MJ and Stephenson DA. Recent developments in neurofibromatosis type 1. Curr Opin Neurol 2007; 20: 135-141.

[3] Tchernev G, Chokoeva AA, Patterson JW, Bakardzhiev I, Wollina U and Tana C. Plexiform neurofibroma: a case report. Medicine 2016; 95: e2663.

[4] Hirbe AC and Gutmann DH. Neurofibromatosis type 1: a multidisciplinary approach to care. Lancet Neurol 2014; 13: 834-843.

[5] Korf BR. Plexiform neurofibromas. Am J Med Genet 1999; 89: 31-37.

[6] Park SY and Kim JS. A short guide to histone deacetylases including recent progress on class II enzymes. Exp Mol Med 2020; 52: 204-212.

[7] Choi JH, Kwon HJ, Yoon BI, Kim JH, Han SU, Joo HJ and Kim DY. Expression profile of histone deacetylase 1 in gastric cancer tissues. Jpn J Cancer Res 2001; 92: 1300-1304.

[8] Halkidou K, Gaughan L, Cook S, Leung HY, Neal DE and Robson CN. Upregulation and nuclear recruitment of HDAC1 in hormone refractory prostate cancer. Prostate 2004; 59: 177-189.

[9] Zhang Z, Yamashita H, Toyama T, Sugiura H, Ando Y, Mita K, Hamaguchi M, Hara Y, Kobayashi S and Iwase H. Quantitation of HDAC1 mRNA expression in invasive carcinoma of the breast*. Breast Cancer Res Treat 2005; 94: 11-16.

[10] Zhu P, Martin E, Mengwasser J, Schlag P, Janssen KP and Göttlicher M. Induction of HDAC2 expression upon loss of APC in colorectal tumorigenesis. Cancer Cell 2004; 5: 455-463.

[11] Zhang Z, Yamashita H, Toyama T, Sugiura H, Omoto Y, Ando Y, Mita K, Hamaguchi M, Hayashi S and Iwase H. HDAC6 expression is correlated with better survival in breast cancer. Clin Cancer Res 2004; 10: 6962-6968.

[12] Bora-Singhal N, Mohankumar D, Saha B, Colin CM, Lee JY, Martin MW, Zheng X, Coppola D and Chellappan S. Novel HDAC11 inhibitors suppress lung adenocarcinoma stem cell self-renewal and overcome drug resistance by suppressing Sox2. Sci Rep 2020; 10: 4722.

[13] Buglio D, Khaskhely NM, Voo KS, Martinez-Valdez H, Liu YJ and Younes A. HDAC11 plays an essential role in regulating OX40 ligand expression in Hodgkin lymphoma. Blood 2011; 117: 2910-2917.

[14] Klieser E, Urbas R, Stättner S, Primavesi F, Jäger T, Dinnewitzer A, Mayr C, Kiesslich T, Holzmann K, Di Fazio P, Neureiter D and Swierczynski S. Comprehensive immunohistochemical analysis of histone deacetylases in pancreatic neuroendocrine tumors: HDAC5 as a predictor of poor clinical outcome. Hum Pathol 2017; 65: 41-52.

[15] Feng W, Lu Z, Luo RZ, Zhang X, Seto E, Liao WS and Yu Y. Multiple histone deacetylases repress tumor suppressor gene ARHI in breast cancer. Int J Cancer 2007; 120: 1664-1668.

[16] Thole TM, Lodrini M, Fabian J, Wuenschel J, Pfeil S, Hielscher T, Kopp-Schneider A, Heinicke U, Fulda S, Witt O, Eggert A, Fischer M and Deubzer HE. Neuroblastoma cells depend on HDAC11 for mitotic cell cycle progression and survival. Cell Death Dis 2017; 8: e2635.

[17] Martin MW, Lee JY, Lancia DR Jr, Ng PY, Han B, Thomason JR, Lynes MS, Marshall CG, Conti C, Collis A, Morales MA, Doshi K, Rudnitskaya A, Yao L and Zheng X. Discovery of novel N-hydroxy-2-arylisoindoline-4-carboxamides as potent and selective inhibitors of HDAC11. Bioorg Med Chem Lett 2018; 28: 2143-2147.

[18] Yue L, Sharma V, Horvat NP, Akuffo AA, Beatty MS, Murdun C, Colin C, Billington JMR, Goodheart WE, Sahakian E, Zhang L, Powers JJ, Amin NE, Lambert-Showers QT, Darville LN, Pinilla-Ibarz J, Reuther GW, Wright KL, Conti C, Lee JY, Zheng X, Ng PY, Martin MW, Marshall CG, Koomen JM, Levine RL, Verma A, Grimes HL, Sotomayor EM, Shao Z and Epling-Burnette PK. HDAC11 deficiency disrupts oncogene-induced hematopoiesis in myeloproliferative neoplasms. Blood 2020; 135: 191-207.

[19] Bora-Singhal N, Mohankumar D, Saha B, Colin CM, Lee JY, Martin MW, Zheng X, Coppola D and Chellappan S. Novel HDAC11 inhibitors suppress lung adenocarcinoma stem cell self-renewal and overcome drug resistance by suppressing Sox2. Sci Rep 2020; 10: 4722.

[20] Lee MJ, Lee JC, Hsieh JH, Lin MY, Shih IA, You HL and Wang K. Cordycepin inhibits the proliferation of malignant peripheral nerve sheath tumor cells through the p53/Sp1/tubulin pathway. Am J Cancer Res 2021; 11: 1247-1266.

[21] Johansson G, Mahller YY, Collins MH, Kim MO, Nobukuni T, Perentesis J, Cripe TP, Lane HA, Kozma SC, Thomas G and Ratner N. Effective in vivo targeting of the mammalian target of rapamycin pathway in malignant peripheral nerve sheath tumors. Mol Cancer Ther 2008; 7: 1237-1245.

[22] Miller SJ, Rangwala F, Williams J, Ackerman P, Kong S, Jegga AG, Kaiser S, Aronow BJ, Frahm S, Kluwe L, Mautner V, Upadhyaya M, Muir D, Wallace M, Hagen J, Quelle DE, Watson MA, Perry A, Gutmann DH and Ratner N. Large-scale molecular comparison of human schwann cells to malignant peripheral nerve sheath tumor cell lines and tissues. Cancer Res 2006; 66: 2584.

[23] Johansson G, Peng PC, Huang PY, Chien HF, Hua KT, Kuo ML, Chen CT and Lee MJ. Soluble AXL: a possible circulating biomarker for neurofibromatosis type 1 related tumor burden. PLoS One 2014; 9: e115916.

[24] Al Shoyaib A, Archie SR and Karamyan VT. Intraperitoneal route of drug administration: should it be used in experimental animal studies? Pharm Res 2019; 37: 12.

[25] Wu LMN, Deng Y, Wang J, Zhao C, Wang J, Rao R, Xu L, Zhou W, Choi K, Rizvi TA, Remke M, Rubin JB, Johnson RL, Carroll TJ, Stemmer-Rachamimov AO, Wu J, Zheng Y, Xin M, Ratner N and Lu QR. Programming of schwann cells by Lats1/2-TAZ/YAP signaling drives malignant peripheral nerve sheath tumorigenesis. Cancer Cell 2018; 33: 292-308, e297.

[26] Anbanandam A, Albarado DC, Nguyen CT, Halder G, Gao X and Veeraraghavan S. Insights into transcription enhancer factor 1 (TEF-1) activity from the solution structure of the TEA domain. Proc Natl Acad Sci U S A 2006; 103: 17225-17230.

[27] Shreberk-Shaked M and Oren M. New insights into YAP/TAZ nucleo-cytoplasmic shuttling: new cancer therapeutic opportunities? Mol Oncol 2019; 13: 1335-1341.

[28] Gao L, Cueto MA, Asselbergs F and Atadja P. Cloning and functional characterization of HDAC11, a novel member of the human histone deacetylase family. J Biol Chem 2002; 277: 25748-25755.

[29] Dai W, Zeller C, Masrour N, Siddiqui N, Paul J and Brown R. Promoter CpG island methylation of genes in key cancer pathways associates with clinical outcome in high-grade serous ovarian cancer. Clin Cancer Res 2013; 19: 5788-5797.

[30] Deubzer HE, Schier MC, Oehme I, Lodrini M, Haendler B, Sommer A and Witt O. HDAC11 is a novel drug target in carcinomas. Int J Cancer 2013; 132: 2200-2208.

[31] Gumbarewicz E, Luszczki JJ, Wawruszak A, Dmoszynska-Graniczka M, Grabarska AJ, Jarzab AM, Polberg K and Stepulak A. Isobolographic analysis demonstrates additive effect of cisplatin and HDIs combined treatment augmenting their anti-cancer activity in lung cancer cell lines. Am J Cancer Res 2016; 6: 2831-2845.

[32] Wei Y, Guo Y, Zhou J, Dai K, Xu Q and Jin X. Nicotinamide overcomes doxorubicin resistance of breast cancer cells through deregulating SIRT1/Akt pathway. Anticancer Agents Med Chem 2019; 19: 687-696.

[33] Zhou L, Jilderda LJ and Foijer F. Exploiting aneuploidy-imposed stresses and coping mechanisms to battle cancer. Open Biol 2020; 10: 200148.

[34] Sui L, Zhang S, Huang R and Li Z. HDAC11 promotes meiotic apparatus assembly during mouse oocyte maturation via decreasing H4K16 and alpha-tubulin acetylation. Cell Cycle 2020; 19: 354-362.

[35] Mayr MI, Hummer S, Bormann J, Gruner T, Adio S, Woehlke G and Mayer TU. The human kinesin Kif18A is a motile microtubule depolymerase essential for chromosome congression. Curr Biol 2007; 17: 488-498.

[36] Zanconato F, Cordenonsi M and Piccolo S. YAP/TAZ at the roots of cancer. Cancer Cell 2016; 29: 783-803.

[37] Lau AN, Curtis SJ, Fillmore CM, Rowbotham SP, Mohseni M, Wagner DE, Beede AM, Montoro DT, Sinkevicius KW, Walton ZE, Barrios J, Weiss DJ, Camargo FD, Wong KK and Kim CF. Tumor-propagating cells and Yap/Taz activity contribute to lung tumor progression and metastasis. EMBO J 2014; 33: 468-481.

[38] Cordenonsi M, Zanconato F, Azzolin L, Forcato M, Rosato A, Frasson C, Inui M, Montagner M, Parenti AR, Poletti A, Daidone MG, Dupont S, Basso G, Bicciato S and Piccolo S. The Hippo transducer TAZ confers cancer stem cell-related traits on breast cancer cells. Cell 2011; 147: 759-772.

[39] Huh HD, Kim DH, Jeong HS and Park HW. Regulation of TEAD transcription factors in cancer biology. Cells 2019; 8: 600.

[40] Bai N, Zhang C, Liang N, Zhang Z, Chang A, Yin J, Li Z, Luo N, Tan X, Luo N, Luo Y, Xiang R, Li X, Reisfeld RA, Stupack D, Lv D and Liu C. Yes-associated protein (YAP) increases chemosensitivity of hepatocellular carcinoma cells by modulation of p53. Cancer Biol Ther 2013; 14: 511-520.

[41] Engeland K. Cell cycle arrest through indirect transcriptional repression by p53: i have a dream. Cell Death Differ 2018; 25: 114-132.

[42] Holtkamp N, Atallah I, Okuducu AF, Mucha J, Hartmann C, Mautner VF, Friedrich RE, Mawrin

C and von Deimling A. MMP-13 and p53 in the progression of malignant peripheral nerve sheath tumors. Neoplasia 2007; 9: 671-677.

[43] Holtkamp N, Malzer E, Zietsch J, Okuducu AF, Mucha J, Mawrin C, Mautner VF, Schildhaus HU and von Deimling A. EGFR and erbB2 in malignant peripheral nerve sheath tumors and implications for targeted therapy. Neuro Oncol 2008; 10: 946-957.

[44] Wang W, Fu L, Li S, Xu Z and Li X. Histone deacetylase 11 suppresses p53 expression in pituitary tumor cells. Cell Biol Int 2017; 41: 1290-1295.

[45] Koo JH and Guan KL. Interplay between YAP/TAZ and metabolism. Cell Metab 2018; 28: 196-206.